Indocyanine green uptake by human tumor and non-tumor cell lines and tissue

HOANG-NGAN NGUYEN*, DAVID PERTZBORN*, RAFAT ZIADAT, GÜNTHER ERNST, ORLANDO GUNTINAS-LICHIUS, FERDINAND VON EGGELING and FRANZISKA HOFFMANN

Working Group Innovative Biophotonics, Department of Otorhinolaryngology, Jena University Hospital, D-07747 Jena, Germany

Received May 14, 2024; Accepted July 2, 2024

DOI: 10.3892/br.2024.1824

Abstract. Indocyanine green (ICG) is a potential promising dye for a better intraoperative tumor border definition and an improved patient outcome by potentially improving tumor border visualization compared with traditional white light guided surgery. Here, the cellular uptake of ICG in human squamous cell carcinoma (SCC026) and immortalized non-cancer skin (HaCaT) cell lines was evaluated to study the tumor-specific cellular uptake of ICG. The spatial distribution of ICG inside tumor tissue was investigated in tissue sections of head and neck squamous cell carcinoma at a microscopic level. ICG uptake and internalization was observed in living cells after 2.5 h and in the nucleus after 24 h. In dead cells, higher and faster uptake was observed. In the tissue sections, higher ICG signal intensity could be detected in connective tissue and surrounding clusters and blood vessels. In conclusion, no distinct ICG uptake by tumor cells was detected in cancer cell lines and tumor tissue. ICG localization in certain regions of tumor tissue appears to be a result of enhanced tissue permeability and retention, but not specific to tumor cells.

Introduction

A clear intraoperative tumor border definition is essential for complete tumor resection and strongly improves patient outcomes (1). The intraoperative evaluation of tumor borders is performed by visual inspection followed by histological analysis. This procedure is error-prone and time-consuming. Evolving imaging techniques allow better visualization of the operation field in real-time. One such technique is near-infrared (NIR) fluorescence-guided surgery (2,3). Fluorophores are used as contrast agents. Indocyanine green (ICG) has been approved by the Food and Drug Administration and European Medicine Agency. It is widely used in diagnostic medical imaging for perfusion and angiographic applications (4,5). Additionally, due to its advantages such as long retention time and higher signal-to-noise ratio compared with other fluorophores, its potential use is still under investigation in biomedical research (6,7).

Several studies have shown an association between tumor tissue and ICG signals *in vivo* (8,9). This has led to the introduction of ICG for tumor imaging in several tumor entities (10) with a focus on sentinel lymph nodes (11). One potential use is the visualization of tumor areas in patients with head and neck squamous cell carcinoma (HNSCC) (12), which has low 5-year survival rates of ~50% and may benefit from technologies for better visualization and tumor border definition. In HNSCC failing to fully remove the tumor with adequate margins during surgery is the primary cause of patient death (13). To the best of our knowledge, there has not been any study showing evidence of tumor-specific cellular uptake of ICG in patients, even though results have shown preferential cellular uptake in tumor xenografts; ICG labeling of tumor is indirect and seems to be driven by higher endocytotic activity of tumor cells in combination with the disruption of tight junctions (14). This leads to enhanced permeability and retention (EPR) effect by which macromolecules accumulate in tumor tissue (15). To the best of our knowledge, however, little is known about the histological distribution of ICG following injection in human cancer samples at the microscopic level.

The present study aimed to evaluate the tumor and non-tumor cellular uptake of ICG and its spatial distribution at a microscopic level. A high-magnification imaging approach was used for the detection of ICG in HNSCC cell lines and spatial distribution of ICG within tissue samples from patients with HNSCC.

Materials and methods

Cells and tissue samples. The human squamous cell carcinoma cell line SCC026 [cat. no. ACC-658, Research Resource Identifier (RRID):CVCL_2221] and immortalized human skin cell line HaCaT (RRID:CVCL_0038; cat. no. 300493; passage number of cryopreservation, 31) were obtained from Leibniz

Correspondence to: Professor Ferdinand von Eggeling, Working Group Innovative Biophotonics, Department of Otorhinolaryngology, Jena University Hospital, 1 House A, Am Klinikum, D-07747 Jena, Germany
E-mail: feggeling@med.uni-jena.de

*Contributed equally

Key words: indocyanine green, oral cancer, tumor cell, tumor marker

Institute DSMZ Germany. Growth medium for SCC06 consisted of 80% Eagle's Minimal Essential Medium (Thermo Fisher Scientific, Inc.), 20% fetal bovine serum (Thermo Fisher Scientific, Inc.) and 2 mM L-glutamine. Growth medium for HaCaT consisted of 90% Dulbecco's Modified Eagle's Medium (Thermo Fisher Scientific, Inc.), 10% fetal bovine serum and 2 mM L-glutamine.

Tissue samples from five patients with HNSCC were collected at Jena University Hospital, Jena, Germany between September 2019 and November 2021. The study was approved by the ethics committee of the Jena University Hospital (approval no. 4291-12/14) and written informed consent was obtained from all patients. All patients were male, ranging in age from 61 to 70 years. Exclusion criteria were other malignancies or multimorbidity that prevent surgery, such as advanced patient age, cardiovascular, respiratory, neurological or cognitive impairment and coagulopathy (16). No criterion was applied with regards to sex but due to the sex ratio of head and neck cancer being nearly 4:1 (78.9% male) (17) and the small patient cohort, only male patients were recruited. One sample originated from the oropharynx, two from the oral cavity and two from the larynx. An overview of patients and their clinical data is provided in Table I including TNM cancer staging (18). The samples originated from the tumor area as well as adjacent healthy tissue (distance >5 mm, clear margins). All patients received ICG intravenously during tumor surgery according to a standardized protocol (3). ICG dissolved in distilled water (5 ml; 25 mg/15 ml solution; Pulsion Medical Systems SE, Getinge) was administered intravenously during surgery after anesthesia induction and endoscopic exposure of the tumor. To confirm successful ICG administration near-infrared endoscopy was performed. At 30 min after ICG injection, specimens were collected. The samples were snap frozen in liquid nitrogen and stored at -80˚C until measurement. Sections (12 μm thickness) were cut with a cryotome (Leica Biosystems). Fresh frozen sections were prepared and transported under low light to prevent photo-bleaching.

Fluorescence microscopy. All fluorescence images were captured using an inverted light microscope (Axio Observer Z1/7; Carl Zeiss AG) with a universal LED illumination system (pE-4000; CoolLED Ltd.) and sCMOS camera (ORCA-Fusion BT; Hamamatsu Photonics K.K.) with an 1x camera adapter. Images of cell cultures were captured using a 63x lens (LD Plan-Neofluar 63x/0.75 Korr M27; Carl Zeiss AG). Images of tissue sections were captured using a 40x lens (LD Plan-Neofluar 40x/0.6 Korr M27; Carl Zeiss AG). ICG was detected using the ICG HC filter set (AHF Analysentechnik AG). Ethidium homodimer-1 was detected using a 45 Texas Red filter set (Carl Zeiss AG). Calcein-AM was detected using a 44 FITC filter set (Carl Zeiss AG). Hoechst 33342 was detected using a 96 HE BFP filter set (Carl Zeiss AG). All fluorescence images were shown in pseudo-colors. ZEN 3.5 blue edition imaging software (Carl Zeiss AG) was used for all experiments. For fluorescence intensity in tissue sections, the mean pixel intensity of the corresponding tissue area was calculated and compared using Python software (Version 3.7, Python Software Foundation). Tissue areas including artifacts were identified and removed for the calculation.

SCC026 and HaCaT cells were seeded at a density of $0.1x10^6$ cells/ml on a surface area of 1.9 cm^2/dish. The cells were incubated at 37˚C and 5% CO_2 for 24 h until they reached 70-90% confluence. To investigate ICG uptake, growth medium was removed and fresh medium containing 0.6 μg/ml ICG (Verdye™, Diagnostic Green GmbH) was added. All steps involving ICG or fluorescent agents were performed under low light conditions to prevent photobleaching. Cells were incubated with ICG medium at 37˚C and 5% CO_2 for different time lengths (1, 45 and 90 min, 2.5 and 24.0 h). ICG medium was removed, cells were washed with Dulbecco's Phosphate-Buffered Saline (DPBS; Sigma-Aldrich Chemie GmbH) and fresh growth medium was added. The cells were subjected to ICG fluorescence imaging. To distinguish live from dead cells, cells were stained with calcein AM and ethidium homodimer-1 (both Thermo Fisher Scientific, Inc.). Staining solution consisted of DPBS with $2x10^{-3}$ mM/l calcein AM and $4x10^{-3}$ mM/l ethidium homodimer-1. The medium was removed, the cells were washed with DPBS and 150 μl staining solution was added to the cells. Cells were incubated with the fluorescence staining solution at room temperature for 30 min before fluorescence imaging. The exposure time was automatically determined by the imaging software (ZEN 3.5 blue edition imaging software; Carl Zeiss AG, micro-shop.zeiss.com/de/de/softwarefinder/software-categories/zen-blue). Additionally, a control group of cells underwent the same incubation and staining conditions without treatment with ICG. The influence on the cell survival was judged visually.

SCC026 and HaCaT cells were seeded with a density of $0.075x10^6$ cells/ml on a surface area of 1.9 cm^2/dish. The cells were incubated at 37˚Cand 5% CO_2 for 24 h until they reached 70-90% confluence. To investigate the ICG retention, the cells were incubated at 37˚C with 0.6 μg/ml ICG for 2.5 h. ICG medium was then removed, and fresh growth medium added. The cells were incubated in ICG-free growth medium at 37˚C and 5% CO_2 (0.5, 2.5, 4.0, 4.5, 5.0, 5.5, 6.0 and 24.0 h). To differentiate between cell nucleus and cytoplasm, cells were stained with Hoechst 33342 (Thermo Fisher Scientific, Inc.) and calcein AM. Staining solution consisted of DPBS with $8.115x10^{-3}$ mM/l Hoechst 33342 and $2x10^{-3}$ mM/l calcein AM. The medium was removed, the cells were washed with DPBS and 150 μl staining solution was added to the cells. Cells were incubated with the fluorescence staining solution at room temperature for 30 min before ICG/calcein/Hoechst fluorescence imaging. The exposure time was automatically determined by the imaging software.

ICG fluorescence imaging were performed on fresh frozen sections. Individual images were combined with an overlap of 15% to obtain ICG fluorescence images of the entire tissue section. The exposure time for all images was set at 10 sec. Tissue sections were stained with hematoxylin and eosin (HE; hematoxylin: 5 min, Eosin: 20 sec, at room temperature) after ICG fluorescence imaging and submitted to an experienced pathologist for analysis (including the search for necrotic tissue or cells) and annotation. The annotated HE images were co-registered with the ICG fluorescence images to investigate the distribution of ICG inside the tissue.

Table I. Overview of patients and their clinical data.

Patient	Age, years	Cancer	Tumor localization	TNM (stage)
1	61	Floor of the mouth	Floor of the mouth	pT1(2) cN0c M0 L0 V0 Pn0 R0 (I)
2	54	Floor of the mouth	Floor of the mouth	pT3 pN0(0/24) cM0 L0 V0 Pn0 R0; (II)
3	67	Oropharyngeal	Oropharynx	cT2 cN3b cM0 (III)
4	70	Laryngeal	Vocal fold	cT1a cN0 cM0 (I)
5	61	Laryngeal	Larynx	cT1b cN0 cM0 (I)

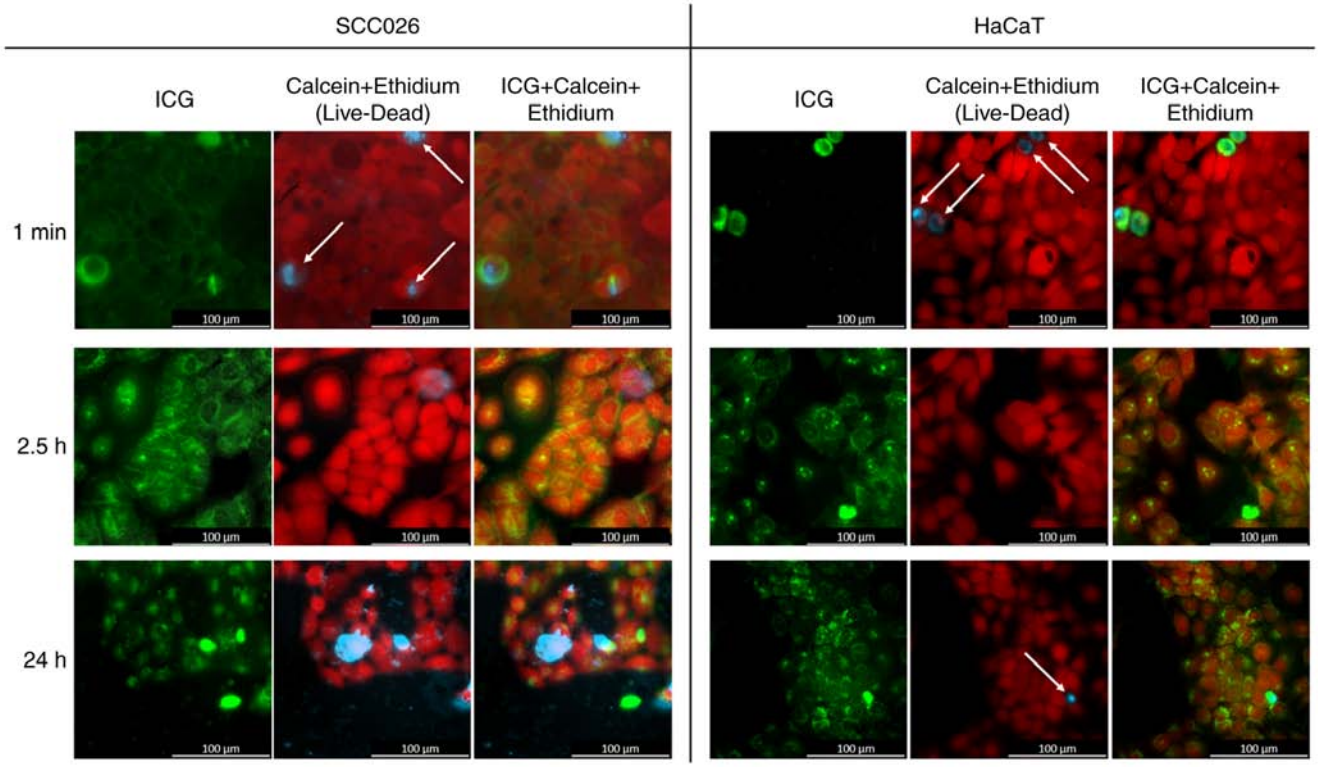

Figure 1. ICG uptake of living cells. SCC026 (tumor cells) and HaCaT (non-tumor cells) were incubated in ICG medium for 1 min, 2.5 h and 24.0 h. Uptake of ICG in dead cells was observed after 1 min and in living cells at 2.5 h. Transport of ICG to the cell nucleus of living cells was observed at 24 h. Arrows indicate dead cells. Green, ICG; red, calcein AM (cytoplasm of living cells); blue, ethidium homodimer-1 (nucleus of dead cells). ICG, Indocyanine green.

Results

ICG imaging of cell cultures. No notable effect of ICG on cell survival was observed. The number of dead cells was similar in the ICG and the control group (data not shown). Uptake of ICG by dead cells was observed after 1 min of incubation in ICG medium. Overall, dead cells showed earlier and higher ICG uptake than living cells (Fig. 1A).

No notable ICG uptake by living cells could be observed for the first 90 min (data not shown). ICG was only detected in the intercellular space and inside dead cells. After 2.5 h, ICG was taken up and internalized by living cells in both cell lines (Fig. 1B). At 24 h, transport to the nucleus of living cells was observed in both cell lines (Fig. 1C).

Imaging of tissue sections. For investigation of the *in vivo* distribution of ICG, samples from patients following ICG injection and surgery were used.

In all tissue sections, ICG distribution was distinctive and not diffuse. Higher ICG signal intensity was detected in connective tissue and surrounding cell clusters (Fig. 2) and cell clusters surrounding blood vessels (Fig. 3). ICG signal intensity was studied in representative samples of connective tissue and healthy epithelium as well as tumor tissue. The signal intensity was higher in connective compared with tumor tissue (Fig. 2A-C) and healthy epithelium (Fig. 2D-F). ICG signal intensity decreased with increasing distance from connective tissue. Higher ICG signal intensity was also detected in the connective tissue of healthy epithelial tissue located in close proximity to tumor tissue (Fig. 2D-F). The higher ICG signals at the section edges were associated with diffusion artifacts from thawing of the tissue during the ICG measurement. This edge-zone was therefore excluded from the analysis. Another artifact resulting from tissue preparation (Fig. 2B and C) was also excluded. Fully resolved microscopic images are provided as a publicly available dataset (19).

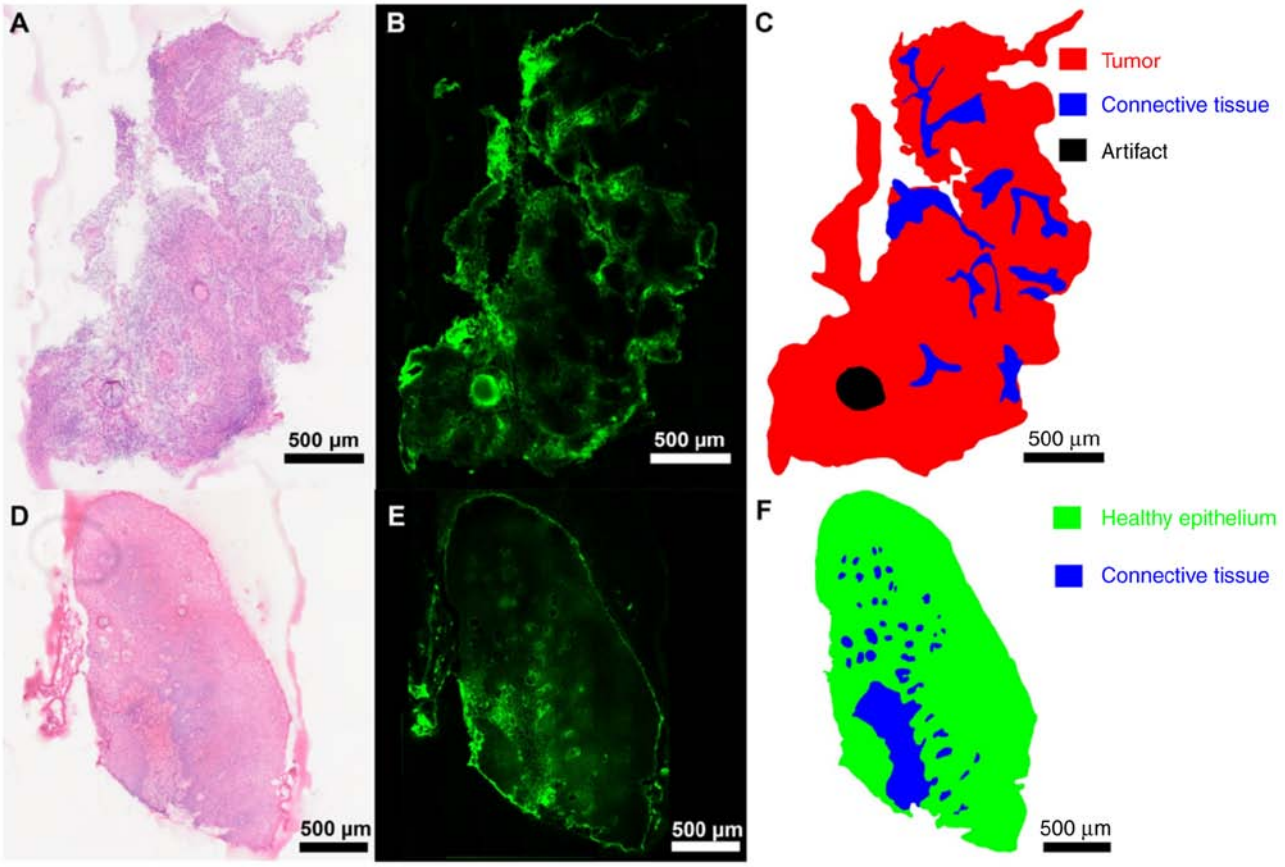

Figure 2. ICG uptake of human tissue. (A) HE staining, (B) ICG fluorescence and (C) histopathological annotation of tumor and connective tissue. (D) HE staining, (E) ICG fluorescence and (F) histopathological annotation of healthy and adjacent connective tissue. HE, hematoxylin and eosin; ICG, Indocyanine green.

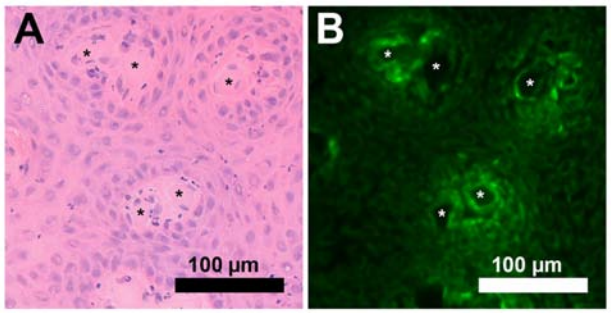

Figure 3. Co-registered images of blood vessels (*) and surrounding cell clusters. Leaking of ICG from the blood vessel and uptake into the cells could be observed in (A) hematoxylin and eosin-stained sections and (B) ICG fluorescence images. ICG, Indocyanine green.

Discussion

ICG angiography is used to examine choroidal blood flow and associated pathologies (20). In tumor surgery, ICG has been introduced in clinical practice to detect sentinel lymph nodes and identify regional metastasis (11,21). Many studies with ICG have been conducted to test its suitability for determining tumor boundaries *in vivo* (22). Accurate labeling of tumor margins would assist during surgery; however studies have not yet been able to clearly show whether this is possible (22,23). Since it is difficult to study ICG distribution during surgery, the aim of the present study was to investigate the application of ICG using cell lines and tissue as model.

Earlier and higher uptake of ICG by dead cells was observed. This was expected, since necrotic cells no longer have a functioning cell barrier, allowing ICG to enter the cell more easily (24). Egloff-Juras *et al* (25) studied the uptake of ICG by living cells in FaDu spheroids with similar results regarding ICGpenetration after 24 h. While measured at slightly different time intervals compared to this study, Egloff-Juras *et al* also observed low ICG uptake in the first hour with increasing uptake after 3 h. However, neither spheroids nor cell cultures possess blood vessels, which limits the relevance of both the present and aforementioned study. Chan *et al* (26) analyzed ICG uptake and retention in sarcoma and breast cancer cell lines; ICG uptake but not retention was associated with proliferation rate of the sarcoma cell lines. Therefore, that for tumor detection in sarcoma surgery, ICG may demonstrate higher utility in high-grade tumors, which display a higher proliferation rate.

To understand the *in vivo* distribution of ICG, studies on tissue from patients who received ICG intravenously were performed. High ICG signals were primarily detected in connective tissue. This indicated a leaking of ICG from blood vessels, which supports the hypothesis of the EPR effect being the cause of ICG accumulation in tumor tissue due to stronger vascularization (27). However, the strongly heterogenous distribution of ICG and the small patient cohort

limits the present findings. Following injection, ICG rapidly binds non-covalently and reversibly to macromolecules such as albumin in the bloodstream (28). Immature tumor vessels with fenestrated endothelia and deficient basement membranes allow extravasation of these macromolecules, while inefficient lymphatic drainage leads to their retention (EPR effect) (10,15). Chan *et al* (26) concluded that the exact mechanisms underlying ICG uptake and retention require further investigation.

Adjacent connective tissue also showed higher ICG signals. The extent of ICG accumulation in adjacent connective tissue requires further investigation. Patients differ in blood volume and concentration of plasma proteins to which ICG binds, resulting in different ICG concentrations in tissue samples. The ICG dosage injected before surgery was applied based on a standardized procedure (3,29). Furthermore, improved ICG injection protocols for distinct clinical application considering time and location of the injections in addition to dose are under development (30). More objective measurements are needed for large-scale multicenter studies. The detection of higher ICG signals in dead cells *in vitro* experiments led to a search for necrotic cells within the tissue. No necrotic cells were detected in the analyzed tissue samples.

ICG signal intensity decreased with increasing distance from the connective tissue, which indicates a concentration gradient towards the periphery. This pattern was consistent across all samples, regardless of the tumor localization. Therefore, it was hypothesized that this pattern may be universal in HNSCC. Using more samples from more patients and comparing the ICG distribution using immunohistochemical staining for more detailed tumor assessment, is required. As in the cell culture experiments, uptake and internalization of ICG into the cell, but not the nucleus, was detected. All samples were collected 30 min after intravenous administration of ICG. ICG thus had a maximum contact time of 30 min with the tissue. By contrast with the cell culture, transport to the cell nucleus was only observed at 24 h. Further studies with later sampling times after ICG administration cohort should be performed in the future to investigate whether transport to the nucleus occurs after a longer time. This is of particular relevance for a better understanding of the mechanism underlying the second window ICG technique, in which high dose ICG is administered 24 h before surgery (31). While this approach has led to promising findings for laparoscopic fluorescence cholangiography, it is less feasible in clinical applications due to practicability concerns (32). These include additional administrative challenges due to the need of treating patients twice, following a strict timeline that is not well aligned with daily clinical routine, as well as additional costs.

ICG should be used as a tag for other markers with tumor-specific labeling to allow a reliable and effective intraoperative detection of tumor boundaries. A future application of ICG may involve coupling to nanoparticles that enable tumor-specific labeling, which is a topic currently under investigation in a multitude of settings (33,34). Another area of investigation is use of ICG to detect colorectal liver metastasis; specific ICG uptake and retention of cholestatic hepatocytes may increase negative tumor margins during surgery (35,36). A recent study showed the potential of ICG as a universal solid tumor marker if the fluorescence lifetime is measured instead of the signal intensity (37) but questioned the validity of ICG fluorescence intensity as a tumor marker.

In conclusion, no distinct uptake of ICG by tumor cells *in vitro* could be observed. Highlighting of tumor tissue when ICG is administered during surgery appears to be a result of the EPR effect, rather than selective uptake by tumor cells and therefore is not reliable enough to be used as a feasible method of tumor border recognition in the clinic.

Acknowledgements

Not applicable.

Funding

The present study was supported by the Thüringer Aufbaubank/European Regional Development Fund (grant no. 2020 FGI 0029), Carl Zeiss Foundation, Virtual Workshop for Digitization in Sciences (grant no. 0563-2.8/738/2) and Coherent Raman Imaging for the molecular study of origin of diseases (EU Horizon 2020-ICT; grant no. 101016923).

Availability of data and materials

The data generated in the present study may be requested from the corresponding author.

Authors' contributions

OGL, FvE and FH conceived the study. Methodology and experiments were performed by DP, HNN, RZ and GE. DP, FvE and FH wrote the manuscript. Review and editing was performed by OGL and DP. The work was supervised by FvE. DP and FvE confirm the authenticity of all the raw data. All authors have read and approved the final manuscript.

Ethics approval and consent to participate

The study was approved by the ethics committee of the Jena University Hospital (approval no. 4291-12/14) and written informed consent was obtained from all patients.

Patient consent for publication

Not applicable.

Competing interests

The authors declare that they have no competing interests.

References

1. Iseli TA, Lin MJ, Tsui A, Guiney A, Wiesenfeld D and Iseli CE: Are wider surgical margins needed for early oral tongue cancer? J Laryngol Otol 126: 289-294, 2012.
2. Dittberner A, Ziadat R, Hoffmann F, Pertzborn D, Gassler N and Guntinas-Lichius O: Fluorescein-Guided panendoscopy for head and neck cancer using handheld probe-based confocal laser endomicroscopy: A pilot study. Front Oncol 11: 671880, 2021.
3. Schmidt F, Dittberner A, Koscielny S, Petersen I and Guntinas-Lichius O: Feasibility of real-time near-infrared indocyanine green fluorescence endoscopy for the evaluation of mucosal head and neck lesions. Head Neck 39: 234-240, 2017.

4. Schaafsma BE, Mieog JS, Hutteman M, van der Vorst JR, Kuppen PJ, Löwik CW, Frangioni JV, van de Velde CJ and Vahrmeijer AL: The clinical use of indocyanine green as a near-infrared fluorescent contrast agent for image-guided oncologic surgery. J Surg Oncol 104: 323-332, 2011.
5. Atallah I, Milet C, Quatre R, Henry M, Reyt E, Coll JL, Hurbin A and Righini CA: Role of near-infrared fluorescence imaging in the resection of metastatic lymph nodes in an optimized orthotopic animal model of HNSCC. Eur Ann Otorhinolaryngol Head Neck Dis 132: 337-342, 2015.
6. Lu CH and Hsiao JK: Indocyanine green: An old drug with novel applications. Tzu Chi Med J 33: 317-322, 2021.
7. Kitai T, Inomoto T, Miwa M and Shikayama T: Fluorescence navigation with indocyanine green for detecting sentinel lymph nodes in breast cancer. Breast Cancer 12: 211-215, 2005.
8. Yokoyama J, Fujimaki M, Ohba S, Anzai T, Yoshii R, Ito S, Kojima M and Ikeda K: A feasibility study of NIR fluorescent image-guided surgery in head and neck cancer based on the assessment of optimum surgical time as revealed through dynamic imaging. Onco Targets Ther 6: 325-330, 2013.
9. Kedrzycki MS, Leiloglou M, Chalau V, Chiarini N, Thiruchelvam PTR, Hadjiminas DJ, Hogben KR, Rashid F, Ramakrishnan R, Darzi AW, *et al*: The impact of temporal variation in indocyanine green administration on tumor identification during fluorescence guided breast surgery. Ann Surg Oncol 28: 5617-5625, 2021.
10. Vahrmeijer AL, Hutteman M, van der Vorst JR, van de Velde CJ and Frangioni JV: Image-guided cancer surgery using near-infrared fluorescence. Nat Rev Clin Oncol 10: 507-518, 2013.
11. Akrida I, Michalopoulos NV, Lagadinou M, Papadoliopoulou M, Maroulis I and Mulita F: An updated review on the emerging role of indocyanine green (ICG) as a sentinel lymph node tracer in breast cancer. Cancers (Basel) 15: 5755, 2023.
12. Cortese S, Kerrien E, Yakavets I, Meilender R, Mastronicola R, Renard S, Leroux A, Bezdetnaya L and Dolivet G: ICG-induced NIR fluorescence mapping in patients with head & neck tumors after the previous radiotherapy. Photodiagnosis Photodyn Ther 31: 101838, 2020.
13. Hinni ML, Ferlito A, Brandwein-Gensler MS, Takes RP, Silver CE, Westra WH, Seethala RR, Rodrigo JP, Corry J, Bradford CR, *et al*: Surgical margins in head and neck cancer: A contemporary review. Head Neck 35: 1362-1370, 2013.
14. Onda N, Kimura M, Yoshida T and Shibutani M: Preferential tumor cellular uptake and retention of indocyanine green for in vivo tumor imaging. Int J Cancer 139: 673-682, 2016.
15. Wu J: The enhanced permeability and retention (EPR) Effect: The significance of the concept and methods to enhance its application. J Pers Med 11: 771, 2021.
16. Lim L, Chao M, Shapiro J, Millar JL, Kipp D, Rezo A, Fong A, Jones IT, McLaughlin S and Gibbs P: Long-term outcomes of patients with localized rectal cancer treated with chemoradiation or radiotherapy alone because of medical inoperability or patient refusal. Dis Colon Rectum 50: 2032-2039, 2007.
17. Dittberner A, Friedl B, Wittig A, Buentzel J, Kaftan H, Boeger D, Mueller AH, Schultze-Mosgau S, Schlattmann P, Ernst T and Guntinas-Lichius O: Gender disparities in epidemiology, treatment, and outcome for head and neck cancer in germany: A population-based long-term analysis from 1996 to 2016 of the thuringian cancer registry. Cancers (Basel) 12: 3418, 2020.
18. Huang SH and O'Sullivan B: Overview of the 8th edition TNM classification for head and neck cancer. Curr Treat Options Oncol 18: 40, 2017.
19. Hoffmann F: S3_dataset_high resolution microscopy images. zip., 2023. https://doi.org/10.6084/m9.figshare.22331380.v1
20. Stanga PE, Lim JI and Hamilton P: Indocyanine green angiography in chorioretinal diseases: Indications and interpretation: An evidence-based update. Ophthalmology 110: 15-21; quiz 22-3, 2003.
21. Sethi HK, Sina EM, Mady LJ and Fundakowski CE: Sentinel lymph node biopsy for head and neck malignancies utilizing simultaneous radioisotope gamma probe and indocyanine green fluorescence navigation. Head Neck 46: 212-217, 2024.
22. De Ravin E, Venkatesh S, Harmsen S, Delikatny EJ, Husson MA, Lee JYK, Newman JG and Rajasekaran K: Indocyanine green fluorescence-guided surgery in head and neck cancer: A systematic review. Am J Otolaryngol 43: 103570, 2022.
23. Belia F, Biondi A, Agnes A, Santocchi P, Laurino A, Lorenzon L, Pezzuto R, Tirelli F, Ferri L, D'Ugo D and Persiani R: The use of indocyanine green (ICG) and near-infrared (NIR) fluorescence-guided imaging in gastric cancer surgery: A narrative review. Front Surg 9: 880773, 2022.
24. Zhang Y, Chen X, Gueydan C and Han J: Plasma membrane changes during programmed cell deaths. Cell Res 28: 9-21, 2018.
25. Egloff-Juras C, Yakavets I, Scherrer V, Francois A, Bezdetnaya L, Lassalle HP and Dolivet G: Validation of a three-dimensional head and neck spheroid model to evaluate cameras for NIR fluorescence-guided cancer surgery. International Journal of Molecular Sciences 22: 1966, 2021.
26. Chan CD, Brookes MJ, Tanwani R, Hope C, Pringle TA, Knight JC and Rankin KS: Investigating the mechanisms of indocyanine green (ICG) cellular uptake in sarcoma. BioRxiv 2021.2004.2005.438013, 2021.
27. Jiang JX, Keating JJ, De Jesus EM, Judy RP, Madajewski B, Venegas O, Okusanya OT and Singhal S: Optimization of the enhanced permeability and retention effect for near-infrared imaging of solid tumors with indocyanine green. Am J Nucl Med Mol Imaging 5: 390-400, 2015.
28. Cherrick GR, Stein SW, Leevy CM and Davidson CS: Indocyanine green: Observations on its physical properties, plasma decay, and hepatic extraction. J Clin Invest 39: 592-600, 1960.
29. Digonnet A, Van Kerckhove S, Moreau M, Willemse E, Quiriny M, Ahmed B, de Saint Aubain N, Andry G and Bourgeois P: Near infrared fluorescent imaging after intravenous injection of indocyanine green during neck dissection in patients with head and neck cancer: A feasibility study. Head Neck 38 Suppl 1: E1833-E1837, 2016.
30. Ahn HM, Son GM, Lee IY, Shin DH, Kim TK, Park SB and Kim HW: Optimal ICG dosage of preoperative colonoscopic tattooing for fluorescence-guided laparoscopic colorectal surgery. Surg Endosc 36: 1152-1163, 2022.
31. Teng CW, Huang V, Arguelles GR, Zhou C, Cho SS, Harmsen S and Lee JYK: Applications of indocyanine green in brain tumor surgery: Review of clinical evidence and emerging technologies. Neurosurg Focus 50: E4, 2021.
32. Boogerd LSF, Handgraaf HJM, Huurman VAL, Lam HD, Mieog JSD, van der Made WJ, van de Velde CJH and Vahrmeijer AL: The best approach for laparoscopic fluorescence cholangiography: Overview of the literature and optimization of dose and dosing time. Surg Innov 24: 386-396, 2017.
33. Egloff-Juras C, Bezdetnaya L, Dolivet G and Lassalle HP: NIR fluorescence-guided tumor surgery: New strategies for the use of indocyanine green. Int J Nanomedicine 14: 7823-7838, 2019.
34. Borlan R, Focsan M, Maniu D and Astilean S: Interventional NIR fluorescence imaging of cancer: Review on next generation of dye-loaded protein-based nanoparticles for real-time feedback during cancer surgery. Int J Nanomedicine 16: 2147-2171, 2021.
35. Achterberg FB, Sibinga Mulder BG, Meijer RP, Bonsing BA, Hartgrink HH, Mieog JSD, Zlitni A, Park SM, Farina Sarasqueta A, Vahrmeijer AL and Swijnenburg RJ: Real-time surgical margin assessment using ICG-fluorescence during laparoscopic and robot-assisted resections of colorectal liver metastases. Ann Transl Med 8: 1448, 2020.
36. Achterberg FB, Bijlstra OD, Slooter MD, Sibinga Mulder BG, Boonstra MC, Bouwense SA, Bosscha K, Coolsen MME, Derksen WJM, Gerhards MF, *et al*: ICG-Fluorescence imaging for margin assessment during minimally invasive colorectal liver metastasis resection. JAMA Netw Open 7: e246548, 2024.
37. Pal R, Lwin TM, Krishnamoorthy M, Collins HR, Chan CD, Prilutskiy A, Nasrallah MP, Dijkhuis TH, Shukla S, Kendall AL, *et al*: Fluorescence lifetime of injected indocyanine green as a universal marker of solid tumours in patients. Nat Biomed Eng 7: 1649-1666, 2023.